International Journal of Engineering

Journal Homepage: www.ije.ir

# Effect of Residual Stress on Failure of Tube-to-tubesheet Weld in Heat Exchangers

G .H. Farrahi*[a], K. Minaii[a], M. Chamani[a], A. H. Mahmoudi[b]

[a] *School of Mechanical Engineering, Sharif University of Technology, Tehran, Iran*
[b] *Mechanical Engineering Department, Bu-Ali Sina University, Hamedan, Iran*

*PAPER INFO*

*Paper history:*
Received 26 November 2018
Received in revised form 12 December 2018
Accepted 03 January 2019

*Keywords*:
*Residual Stress*
*Post Weld Heat Treatment*
*Heat Exchanger*
*Stress Concentration Factor*

*ABSTRACT*

In a shell and tube heat exchanger, the failure of tube-to-tubesheet welds results in high-pressure water jet which erodes the refractory in front of the tubesheet. Finite element method was employed to simulate the welding process and post weld heat treatment (PWHT) to find the factors affecting the failure in tube-to-tubesheet weldments. Residual stresses in two different geometries of tube-to-tubesheet weldment were calculated through uncoupled thermal-structural analysis. The results showed that the values of residual stresses are higher in heat exchanger of site 1 than site 2 due to more weld passes and geometry of connection. Also, the maximum stress in site 1 occurs at the shellside face of tubesheet while it is on the weld toe in site 2. High tensile residual stresses, especially in Site 1, reduce the tubesheet life. Therefore, performing an efficient PWHT is vital. The PWHT simulation indicated that the process designed is effective for both sites by reducing the residual stress significantly. In addition, the effect of stress concentration was examined on both sites. Moreover, the stress concentration factor in site 1 is as twice as in site 2 and it is the main reason for more failures in site 1.

***doi**: 10.5829/ije.2019.32.01a.15*

## 1. INTRODUCTION

The present study aimed to examine two types of tube-to-tubesheet welding joint in two different shell and tube twin heat exchangers which are used to retrieve energy from reformed gas in a petrochemical unit. In this process, gas inlet temperature and absolute pressure are 975°C and 35 bar, respectively. Saturated water with 326°C temperature and 123 bars absolute pressure was passing around the tubes. The hot gas is cooled down to 465°C while passing the tubes and the ratio of steam to water is increased, while the water pressure and temperature remain constant. In the inlet of the heat exchanger, there are layers of refractory to cover the inner surface of tubeside front shell. These layers act as thermal insulators and prevent the heat exchanger body exposure to hot gas. The body temperature would be 150-180°C due to the insulation effect. Thermal insulation layers protect the front tubesheet from the inlet high temperature gas. Ferrules are used at the front of the tubes, which are in contact with hot gas. A layer of ceramic blanket fills the gap between the ferrule and tube. This type of insulation is used to protect the head of the tube against hot gas and consequent metal dusting. Figure 1 illustrates the structure of the heat exchanger of site 1.

Heat exchanger of site 2 is similar to heat exchanger of site 1 in most of operational parameters. 438 tubes with length of 11.33 m and thickness of 8 mm and 376 tubes with length of 11.75 m and thickness of 6 mm are used in heat exchanger sites1 and 2, respectively. In addition in the center of each tubesheet, a bypass pipe with the same lengths of the tubes, equipped with a control valve is installed in order to adjust the outlet temperature of heat exchanger constant to 465°C. Also, two different methods are employed to weld the tubesheet and tubes.

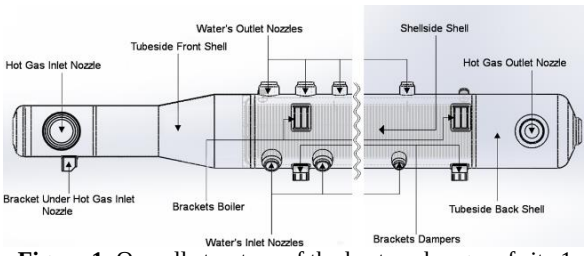


**Figure 1.** Overall structure of the heat exchanger of site 1

*Corresponding Author Email: *farrahi@sharif.edu* (G. H. Farrahi)

Please cite this article as: G. H. Farrahi, K. Minaei, M. Chamani, A. H. Mahmoudi, Effect of Residual Stress on Failure of Tube-to-tubesheet Weld in Heat Exchangers, International Journal of Engineering (IJE), IJE TRANSACTIONS A: Basics Vol. 32, No. 1, (January 2019) 112-120

Figure 2 shows tube-to-tubesheet weldment of sites 1 and 2.

A few researches have been conducted in the field of failure of tube-to-tubesheet weldment. Xu et al. [1] used finite element method to determine the thermo-mechanical stress in tube-to-tubesheet joint for the SCC failure analysis and found that high tensile stress in the tube-to-tubesheet region is the main factor in SCC phenomenon.

The mechanisms of the tubesheet cracking in slurry oil steam generators have been investigated by Zhu et al. [2] using optical and scanning electron microscopy. They observed that the cracks always occurred in the shortest tube–tube ligaments. Mao et al. [3] used a continuum damage mechanics model to calculate the multiaxial fatigue damage of tubesheet of a heat exchanger in steady and transient state and showed that the fatigue damage evolution was significantly accelerated by multiaxial factor. Wei and Ling [4] investigated the effects of four types of tube-to-tubesheet welded structures on mechanical properties and found that extension welded structure have the largest pullout force and fatigue life. Guo et al. [5] showed that intergranular stress corrosion cracking was the main reason for failure of welded 0Cr13Al tube bundle in a heat exchanger. Liu at al. [6] carried out a failure analysis on a tube-to-tubesheet welded joint of a shell and tube heat exchanger and found that this failure was induced by fatigue fracture. Also the causes of cracking in the closing circumferential tube-to-tubesheet welds of five cracked heat exchangers in a petrochemical plant were investigated by Otegui and Fazzini [7]. Luo et al. [8] were studied the effects of repair welding on residual stress in tube to tubesheet connections by finite element method and neutron diffraction measurement and found that repair opposite to the original welding direction minimizes the residual stresses. Also the effects of heat input and welding sequence on residual stresses of tube to tubesheet were studied by Wan et al. [9]. In some other research [10, 11], the failure in tube-to-tubesheet weldment of a heat exchanger is investigated but none of them, has considered the effect of residual stress in failure of tube-to-tubesheet weld. To the best of authors' knowledge, it is the first research that focuses on the effects of residual stress and stress concentration factor in failure of tube-to-tubesheet weldment.

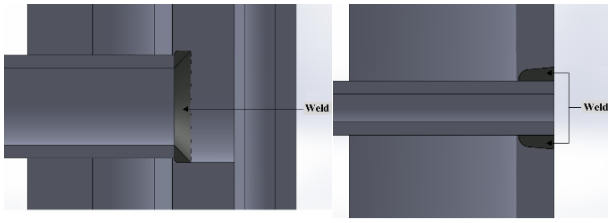


**Figure 2.** Tube-to-tubesheet weldment of sites 1 and 2

In order to find the factors affecting the tube-to-tubesheet joint failure, the welding process and post weld heat treatment were simulated through thermal-structural analysis in sites 1 and 2. In addition, residual stresses were calculated and compared. Given the different failures in sites 1 and 2, the geometry of both joints was examined to select the optimal design after comparing the residual stresses and stress concentration factors. Since the measurment of residual stresses needs special tools, are expensive and time-consuming [12,13], the residual stresses in two heat exchangers were calculated and compared with failures occurred in sites 1 and 2.

## 2. PROBLEM SPECIFICATION

The weld passes of tube-to-tubesheet of both sites are shown in Figure 3. For the joint of site 1 the gap between the tube and tubesheet is filled by multi-pass welding. In the joint of site 2, there is smaller contact area and less passes than site 1. The details of each pass are listed in Table 1, including welding method, speed, voltage, and thickness.

In an overhaul that took place after five years since the start of the operation, after discharging the leaked water in the channels of the heat exchanger, inspections of the tubesheet showed that the welding connection of 6 tubes had been ruptured and, consequently, the hot water had penetrated as a jet into the channel, resulting in the erosion of the tubesheet refractories. Then the tubesheet would be exposed to hot gas at a temperature higher than 900°C and this will cause more damages in the tubesheet.

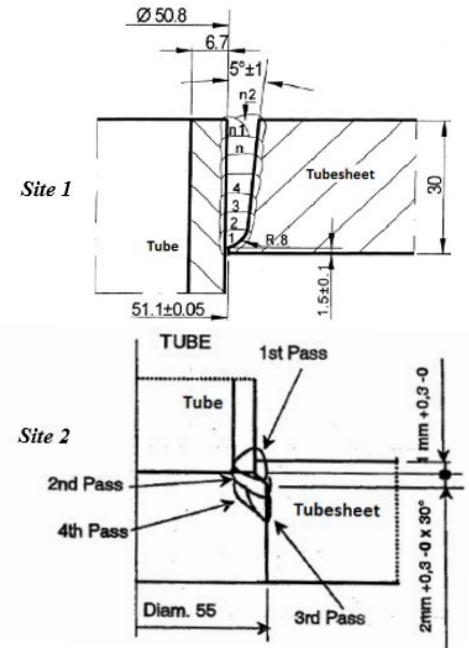


**Figure 3.** Geometry of tube-to-tubesheet welding in site 1 and 2

**TABLE 1.** Information of welding process in sites 1 and 2

| Pass | Site 1 Pass1 | Site 1 Pass 2-7 | Site 1 Pass 8-9 | Site 2 Pass1 | Site 2 Pass 2-4 |
|---|---|---|---|---|---|
| Process | GTAW | GMAW | SMAW | GTAW | GTAW |
| Current (A) | 150 | 200 | 160 | 157.5 | 185 |
| Voltage (V) | 15 | 25 | 25 | 10.5 | 13 |
| Speed (mm/s) | 5 | 3 | 5 | 11.3 | 9.2 |
| Size (mm) | 3 | 3.58 | 4 | 1.1 | 2.5 |

The detached tubes and peripheral cracks on the welding joint are shown in Figusre 4. It should be noted that cracks partly extended to adjacent tubes.

Damage of tube-to-tubesheet resulted in failure of tubesheet refractory and as a consequence, failure of tubesheet. Also, damage of welding joint in site 2 is much lower than site 2. Therefore, it is possible that residual stress or stress concentration are the cause of tube-to-tubesheet failures.

## 3. SIMULATION of WELDING AND PWHT

**3. 1. Welding Simulation** Welding geometries of sites 1 and 2 were modeled in order to compare the tube-to-tubesheet joints. The distances between adjacent tubes in sites 1 and 2 are 80 and 78.75 mm, respectively. Regarding these distances and for reducing the computational time, just one tube was simulated in both sites.

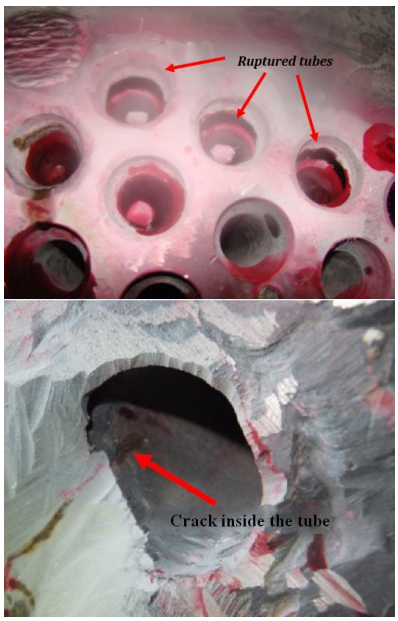


**Figure 4.** Damages of the tubesheet after five years of service

The overall geometry was chosen in such a way that the results of both sites could be compared. The length of tubes, thickness of tubesheet and the edge length in both sites were 300 mm, 30 mm and 300 mm, respectively. The differences between two models were the thickness of tubes, the geometry of welds, and material of tubesheets, which were extracted from technical documents. Half views of the modeled geometries in both sites are presented in Figure 5. In order to simulate the welding process, Abaqus [14] finite element software was utilized.

8-node linear element was used for thermal and structural analysis. The cross sections of the meshing of sites 1 and 2 are shown in Figure 6. Element birth and death technique was used for the modeling of passes. The tubes of both sites were made from the same material, SA 213. The tubesheet of sites 1 and 2 were made from SA 387 and SA 508, respectively.

An elastic-plastic material model with bilinear kinematic as the hardening rule was implemented in structural analysis. All the material constants were defined as to be temperature dependent. Creep model was used in the simulation of PWHT process. The power law applied here is presented in the form of Equation (1) where $\dot{\varepsilon}^{cr}$ is the creep strain rate, $\sigma$ is the uniaxial equivalent deviatoric stress, t is the total time and A, m, n are user defined material dependent properties. Creep-deflection curves are necessary for the calibration of the constants. Krompholz and Kalkhof [15] studied the creep behaviour of SA 508 in 700, 800 and 900 °C. The PWHT has been applied at 650°C. Therefore, the curves have been interpolated to find the power law constants of SA 508 at 650°C. Kimura et al. [16] investigated the creep behavior of SA 213 in 550°C and presented the creep-deflection diagrams. Yagi et al. [17] suggested that the creep behavior of SA 213 and SA 387 are similar. Therefore, similar constants needed to be applied. The calculated constants of power law for different materials are presented in Table 2. The units were calibrated according to Pa for stress and second for time.

Convection boundary condition was applied at the boundaries of the model. For this purpose, we supposed ambient temperature of 25°C and convection coefficient of 10W/m$^2$K for air. According to welding procedure specification (WPS), both sites needs preheat treatment, which was applied by electrical resistance method.

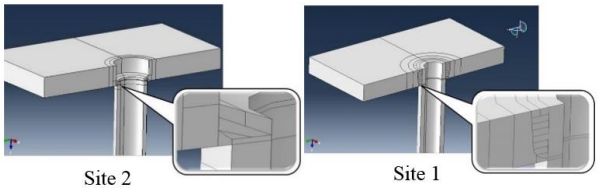


**Figure 5.** Simulation of welding junction of tube-to-tubesheet in sites 1 and 2

Preheat temperatures are 100 and 150°C for sites 1 and 2, respectively. This condition was also applied in the simulation. In order to apply the heat source in the simulation, user defined subroutine DFlux was employed. In this subroutine, the heat source could be defined as a function of position and time. The heat source used in the welding simulation was the Goldak model [18]. This model is a combination of two ellipses: one in the front quadrant of the heat source and the other in the rear quadrant. The heat source should be moved according to the welding speed. This process needs to be consistent with the birth of elements.

$$\dot{\varepsilon}^{cr} = A\sigma^n t^m \quad (1)$$

**3. 2. Pwht Simulation** PWHT is required for tube-to-tubesheet welds. The process of PWHT was documented for the welding in both sites. According to the WPS of tube-to-tubesheet welds, heat treatment was not needed to perform immediately after the welding. Therefore, it is possible to reduce the temperature of parts using air convection for a period of 1000 s and the PWHT was then performed on the tube-to-tubesheet welds. In Table 3, the rate of heating, hold time and temperature and rate of cooling extracted from the WPS are presented for both sites.

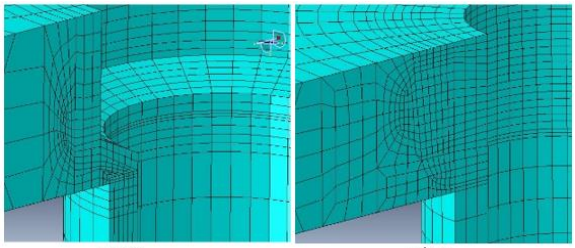


**Figure 6.** Cross section of the meshed models for site 1 and 2

**TABLE 2.** Power law constants for different materials

| Material | A | n | m | Ref. |
|---|---|---|---|---|
| SA 213 Gr.T11 | $2.789 \times 10^{-35}$ | 3.7813 | -0.75 | [17] |
| SA 508 Gr.22 Cl.3 | $6.2766 \times 10^{-16}$ | 1.3916 | -0.2808 | [15] |
| SA 387 Gr.11 Cl.2 | $2.789 \times 10^{-35}$ | 3.7813 | -0.75 | [17] |

**TABLE 3.** PWHT properties of sites 1 and 2

| | Site 1 | Site 2 |
|---|---|---|
| Heating rate (ºC/h) | 186 | 80 |
| Holding time (h) | 1.5 | 1 |
| Temperature (°C) | 630 | 650 |
| Cooling rate (ºC/h) | 220 | 60 |

## 4. RESULT AND DISCUSSIONS

**4. 1. Residual Stress Effect** Temperature distributions in filling process of the welding groove and the motion of thermal flux in site 1 are shown in Figure 7. The maximum temperature in thermal analysis was around 1380°C. Front and rear ellipsoidals of Goldak model are evident in this figure.

Stress distribution on different paths is investigated which is shown in Figure 8. Path 1 is defined on the shellside face of tubesheet, exposed to water, path 2 in the middle of the tubesheet, path 3 on the tubeside face of the tubesheet that is in contact with the refractory, path 4 on the inner surface of the tube, and path 5 on the outer surface of the tube. These five paths are selected in such a way to completely define the distribution of residual stress on the tube-to-tubesheet joint, as the surfaces of the tubesheet and its thickness were defined using path 1, 2, and 3. In addition, the stress distribution on the outer and inner surfaces of the tubes could also be examined using path 4 and 5.

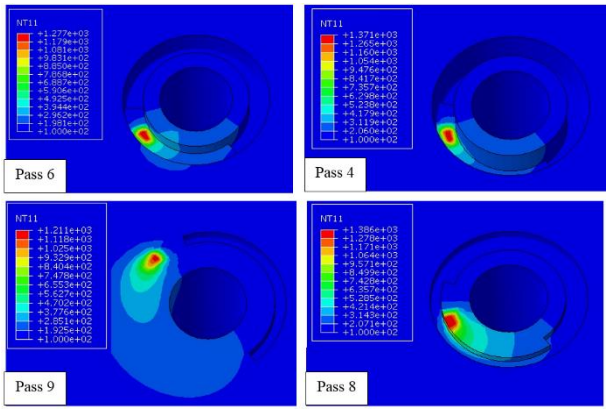


**Figure 7.** Temperature distribution in filling process of the welding groove in site 1

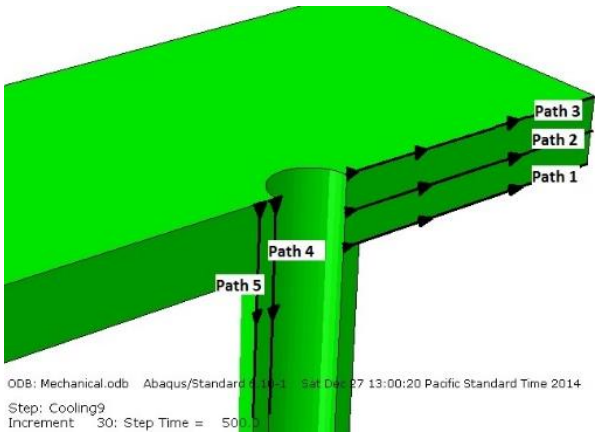


**Figure 8.** Defined paths for investigation of residual stress

Residual stresses are named according to the coordinate system presented in Figure 8. Subscripts 11, 22, and 33 represent x, y, and z directions, respectively. Von Misses stress is also included in the results. It should be noted that the S22 is perpendicular to the shear plane and represents the hoop stress. Paths 4 and 5 in site 2 start from the weld toe while the same paths start on the tubesheet in site 1. For this reason, the results for path 4 and 5 in site 2 are shifted so that they could be compared regarding the tubesheet surface

The distribution of Von Misses stress on the five paths is shown in Figure 9. As expected, the residual stresses reduce with the increasing distance from the weld toe, and converge to zero. On path 2 and 3, the residual stress of site 2 is much lower than of site 1, while the results on path 1 are closer and have a shift in respect to weld toe, because path 1 is closer to the welding toe in site 2. Paths 4 and 5 in site 2 start from the weld toe and continue throughout the tube. Farther away from the weld toe, the stress significantly decreases due to the material change in the tube. A focus on the stresses on path 4 and 5 indicated that the stress on the weld toe in site 2 is much higher than in site 1, and it decreases sharply as it approaches the tube.

Also, the rate of reduction of residual stress along the tubes is similar for both sites due to the fact that the tube materials are similar. In the graphs of site 1 and on path 1-3, a jump is seen, that is related to the change of the material, since the yield stress of the tubesheet is more than the tubes. As shown in Figure 9, the residual stress decreased significantly with performing heat treatment, and the stress decreased over all the directions. An important result seen in these graphs is the uniform stress distribution after the heat treatment.

In Figure 10, the distribution of residual stress in the x direction is compared in different paths for heat exchangers of sites 1 and 2. The stress on paths 4 and 5 is low for both sites. On path 3, this stress component is much lower than site 1 similar to the other stress components on path 3. There are some jumps seen on the different paths. As mentioned before, the jumps are generally created due to material changes from tube-to-tubesheet. Since the yield stress of the tubesheet is higher, the stress increases and then decreases by moving along the tube.

The S22 stress component, which is perpendicular to the shear plane, is compared for sites 1 and 2 in Figure 11. This component decreases as the distance increases from the welding area, and it is significant near the welding toe. On paths 2 and 3, S22 is less in site 2 than site 1, while the S22 on path 1 are closer to each other. On the paths 4 and 5, which include the inner and outer surface of the tubes, the distribution of S22 is similar. The residual stress component of the S33 is similar in both sites and is much lower than the other stress components. Therefore, it is not necessary to report them.

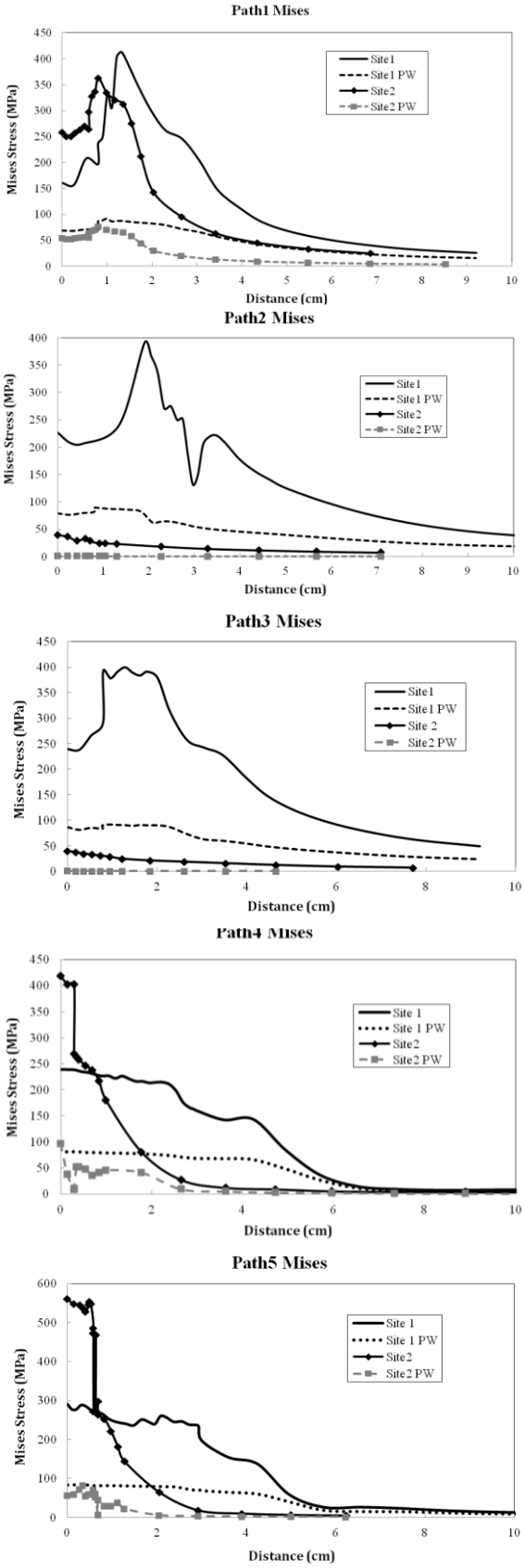


**Figure 9.** Von Misses stress in sites 1 and 2 on paths 1-5

In all diagrams, stress components tend to a low value after the distance of 50 mm. Since the distance between two tubes is 80 mm in site 1 and 78.75 mm in site 2, the stresses on a tube weld do not affect the stress of the adjacent tubes. In other words, considering only one tube in the welding process simulation resulted in enough accuracy for examining the residual stress. There are also tensile stresses in the welding area, which makes the tube and tubesheet highly vulnerable to stress corrosion cracking.

In site 1, the tubesheet is wholly affected by high temperature gradients causing a high residual stress on paths 1, 2 and 3. In contrast, the different passes are such in site 2 that only one small part of the tubesheet is affected by high gradient temperature. Hence, the residual stresses on paths 2 and 3 are much lower in site 2 and maximum stress in path 1 in site 1 are higher than site 2. In site 1, 30 mm of the tube is placed inside the tubesheet. Paths 4 and 5 represent the stress distribution in this region. The stress is constant through this length and tends to zero after that. In site 2, the stress on the weld toe is high but decreases rapidly. In both sites, the rate of residual stress reduction is similar when further from weld toe. This is due to the fact that the material used for the tubes is similar in both heat exchangers. Residual stresses after PWHT could be considered as the main factor in failure of tube-to-tubesheet weldment. As shown in Figures 9-11 in all paths, after PWHT, residual stresses in site 2 are lower than site 1.

### 4. 2. The Effect of Stress Concentration in Welds

In order to examine the strength of the welds, the effect of stress concentration needs to be investigated. In this analysis, a tension force was applied on tube and the maximum stress was calculated. Figure 12 illustrates the stress concentration areas in sites 1 and 2. The area with maximum stress is marked in red. According to Figure 12, the maximum stress in site 1 is on the tubesheet, while it is on the weld toe near the tubesheet in site 2.

As shown in Figures 9 and 11, maximum stresses on Path 1 in site 1 were occurred near the intersection of outer surface of tubes with tubesheet. In this location stress concentration and residual stress is high and could resulted in crack initiation and growth. Different tensile stresses were applied to the tubes and maximum stresses corresponding to these stresses were calculated. In Figure 13, the maximum stress versus applied stress is drawn. The slope of the curves represents the stress concentration factor, which is equal to 3.132 for site 1 and 1.71 for site 2. Therefore, the effect of stress concentration in site 1 is larger than site 2.

## 5. CONCLUSION

The present study examined two different heat exchangers in a petrochemical unit. Using Goldak model

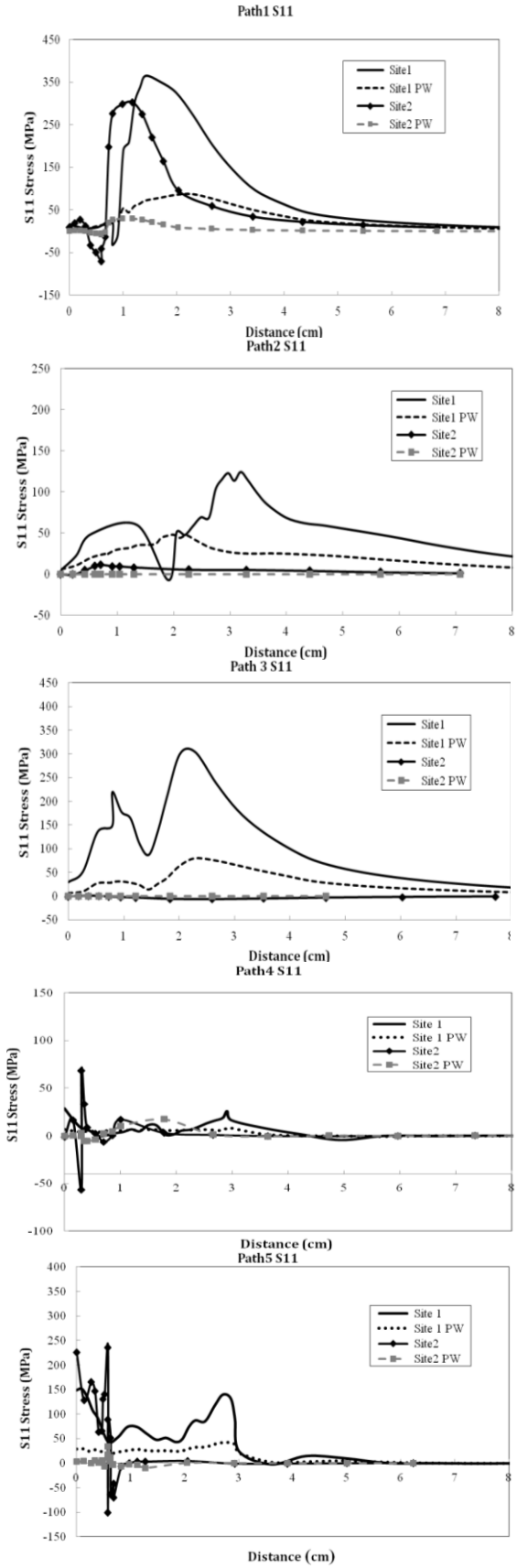


**Figure 10.** S11 stress in sites 1 and 2 on paths 1-5

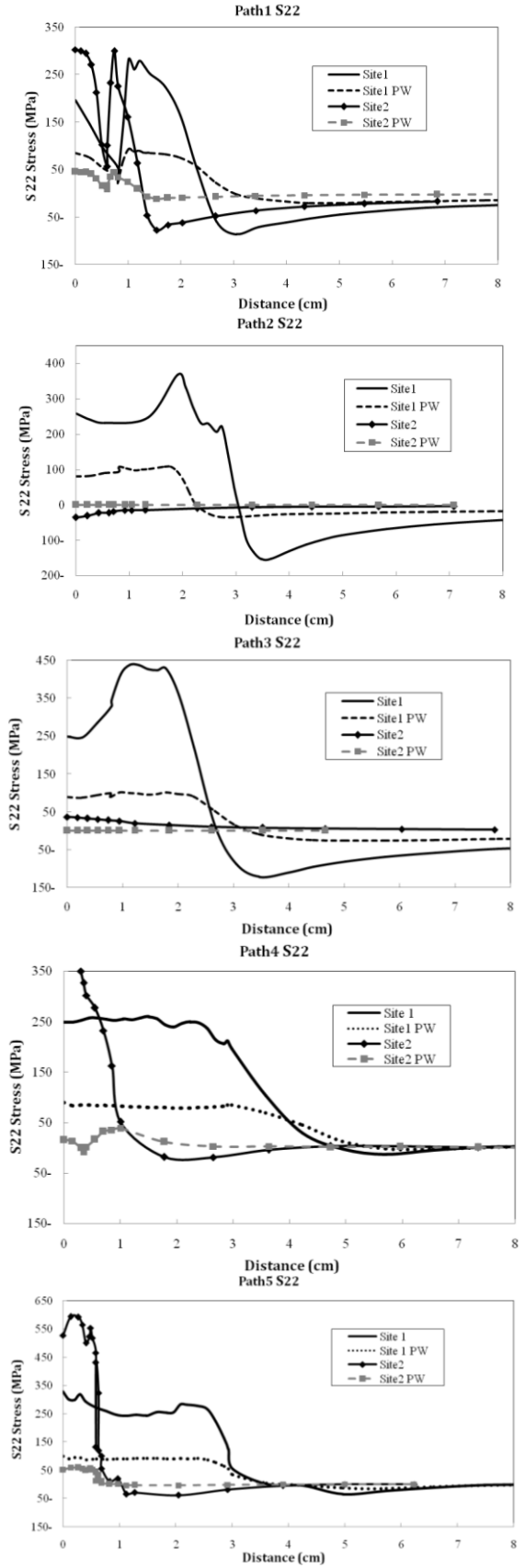


**Figure 11.** S22 stress in sitsses 1 and 2 on paths 1-5

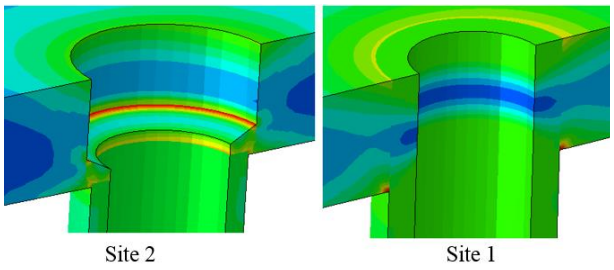


**Figure 12.** Stress concentration areas in sites 1 and 2

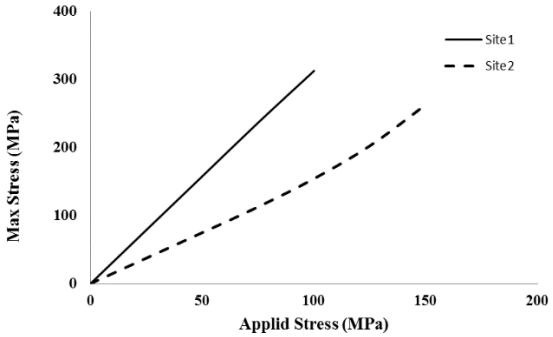


**Figure 13**. Max stress vs. applied stress for sites 1 and 2

as the heat source, temperatures of tube-to-tubesheet connections were calculated and temperature history was used in mechanical analysis. Residual stresses were compared on five paths in tube-to-tubesheet weldment. It is found that the residual stresses in heat exchanger of site 1 were higher than site 2 due to more number of the welding passes applied in site 1 and geometry of weld toe. Residual stress distribution on the surface of tubeside face of tubesheet in site 2 was lower than of site 1. Residual stresses of site 1 on this area are tensile, which will accelerate the cracking process. It is clear that the residual stresses in sites 1 and 2 are of the same range on path 1while the residual stress in site 2 is very low on paths 2 and 3. Where paths 1, 2 and 3 are shellside face of tubesheet, middle of tubesheet and tubeside face of tubesheet respectively. An overall comparison indicates that the welding process of site 1 will create higher tensile residual stresses on the tubesheet and tubes.

Given the high tensile residual stresses, the PWHT seemed to be necessary. The PWHT simulation revealed that the PWHT designed for both sites reduced the residual stresses significantly. This process also reduced the tensile stresses of site 2 on the weld toe. Also, we found that creep has an important effect on relieving of residual stress in PWHT. Comparing residual stresses before and after PWHT, it is found that PWHT must be done precisely and any kind of negligence in performing PWHT will result in harmful consequences.

The examination of the stress concentration effect showed that the maximum stress of site 1 occurred on the

shellside of the tubesheet, while it occurred on the weld toe in site 2. It was also found that the stress concentration was more in site 1 than site 2.

In tube-to-tubesheet joint of site 1, whole thickness of tubesheet is affected by weld passes and since the number of weld passes in site 1 is more than site 2, the possibility of creating defects in weldment of site 1 is more than site 2. Also residual stresses after PWHT in site 2 is more effective than site 1 and value of stresses is much lower. Moreover, stress concentration factor of site 1 is twice of site 2. All of these factors contributed to the less failure in tube-to-tubesheet weldment of site 2 in respect to site 1.

## 6. REFERENCES


1. Xu, S. and Zhao, Y., "Using FEM to determine the thermo-mechanical stress in tube to tubesheet joint for the SCC failure analysis", ***Engineering Failure Analysis,*** Vol. 34, (2013), 24–34.
2. Zhu, L.K., Qiao, L.J., Li, X.Y., Xu, B.Z., Pan, W., Wang. L. and Volinsky, A. A., "Analysis of the tube-sheet cracking in slurry oil steam generators", ***Engineering Failure Analysis,*** Vol. 34, (2013), 379–386.
3. Mao, J., Tang, D., Bao, S., Luo, L. and Gao, Z., "High temperature strength and multiaxial fatigue life assessment of a tubesheet structure", ***Engineering Failure Analysis***, Vol. 68, (2016), 10–21.
4. Wei, X.L. and Ling, X., "Investigation of welded structures on mechanical properties of 304L welded tube-to-tubesheet joints", ***Engineering Failure Analysis***, Vol. 52, (2015), 90-96.
5. Guo, C., Han, C.J., Tang, Y.M., Zuo, Y. and Lin, S.Z., "Failure analysis of welded 0Cr13Al tube bundle in a heat exchanger", ***Engineering Failure Analysis***, Vol.18, (2011), 890–894.
6. Liu, L., Ding, N., Shi, J., Xua, N., Guo, W. and Wu, C. L., "Failure analysis of ***tube***-to-tubesheet welded joints in a shell-tube heat exchanger", ***Case Studies in Engineering Failure Analysis***, Vol.7, (2016), 32–40.
7. Otegui, J.L. and Fazzini, P.G., "Failure analysis of tube–tubesheet welds in cracked gas heat exchangers", ***Engineering Failure Analysis***, Vol.11, (2004), 903–913.
8. Luo, Y., Jiang W., Chen, D., Wimpory, R. C., Li, M. and Liu, X., "Determination of repair weld residual stress in a tube to tube-sheet joint by neutron diffraction and the finite element method", ***ASME Journal of Pressure Vessel Technology***, Vol.140, (2018), 021404-021404-8.
9. Wan, Y., Jiang, W. and Luo Y., "Using X-ray diffraction and FEM to analyze residual stress of tube-to-tubesheet welded joints in a shell and tube heat exchanger", ***ASME Journal of Pressure Vessel Technology***, Vol.139, (2017), 051405-051405-8.
10. Li, H.F., Qian, C.F. and Yuan, Q.B., "Cracking simulation of a tubesheet under different loadings", ***Theoretical and Applied Fracture Mechanics***, Vol. 54, (2010), 27–36.
11. Azevedo, C.R.F., Beneduce Neto, F., Brandi, S.D. and Tschiptschin, A.P., "Cracking of 2.25Cr–1.0Mo steel tube/stationary tube-sheet weldment of a heat-exchanger", ***Engineering Failure Analysis***, Vol.15, (2008), 695–710.
12. Farrahi, G.H., Majzoobi,G.H., Mahmoudi, A.H.and Habibi, N., "Fatigue life of repaired welded tubular joints", ***International Journal of Engineering Transactions A: Basics***, Vol. 26, (2013), 25-32.
13. Mahmoudi, A.H., Hosseinzadeh, A. R. and Jooya, M., "Plasticity effect on residual stresses measurment using contour method", ***International Journal of Engineering Transactions A: Basics***, Vol. 26, (2013), 1203-1212.
14. Abaqus, Analysis user's manual version 6.14, Dassault Systems Simulia Corp., Providence, U.S.A. 2014.
15. Krompholz, K. and Kalkhof, D., "Size effect studies of creep behavior of a pressure vessel steel at temperature from 700 to 900 ºC", ***Journal of Nuclear Materials***, Vol. 305, (2002), 112-123.
16. Kimura, K., Kushima, H., Baba, E., Shimizu, T., Asai, Y., Abe, F. and Yagi, K., "effect of initial microstructure on long term creep strength of a low alloy ferritic steel", ***Testu-to-Hange***, Vol. 86, (2000), 542-549.
17. Yagi, K., Merckling, G., Kern, T.U., Irie, H. and Warlimont, H., "Creep properties of heat resistant steels and superalloys", Landolt Bornstein numerical data & functional relationships in science & technology, ***Springer***, 2nd editions, (2004).
18. Goldak, J., Chakravarti, A. and Bibby, M., "A new finite element model for welding heat sources", ***Metallurgical Transactions B***, Vol. 15, (1984), 299-305.

# Effect of Residual Stress on Failure of Tube-to-tubesheet Weld in Heat Exchangers

G. H. Farrahi[a], K. Minaii[a], M. Chamani[a], A. H. Mahmoudi[b]

[a] *School of Mechanical Engineering, Sharif University of Technology, Tehran, Iran*
[b] *Mechanical Engineering Department, Bu-Ali Sina University, Hamedan, Iran*

*P A P E R I N F O*

*Paper history:*
Received 26 November 2018
Received in revised form 12 December 2018
Accepted 03 January 2019

*Keywords*:
*Residual Stress*
*Post Weld Heat Treatment*
*Heat Exchanger*
*Stress Concentration Factor*

**چکیده**

در یک مبدل حرارتی پوسته و لوله خرابی در اتصال جوشی لوله به تیوب‌شیت منجر به ایجاد جت آب پرفشار می‌شود که سبب خرابی عایق مقابل تیوب شیت می‌گردد. جهت بررسی دلایل ایجاد این خرابی، اتصال جوشی لوله به تیوب شیت و عملیات حرارتی بعد از جوشکاری با استفاده از روش المان محدود مدلسازی شده است. با انجام تحلیل حرارتی–سازه‌ای غیرکوپل تنش‌های پسماند و اعوجاج لوله و تیوب شیت در دو مبدل حرارتی با هندسه اتصال لوله به تیوب شیت متفاوت محاسبه گردید. با بررسی و مقایسه تنش‌های پسماند در هر دو سایت مشخص شد که تنش پسماند در مبدل سایت ۱ بیشتر از سایت ۲ بوده که ناشی از تعداد پاس‌های بیشتر و هندسه اتصال است. همچنین بیشینه تنش در سایت ۱ روی سطح تیوب شیت و در سمت لوله‌ها روی می‌دهد در حالی که در سایت ۲ در محل گرده جوش بیشینه تنش مشاهده میشود. مقادیر بالای تنش پسماند کششی خصوصا در سایت ۱ عمر تیوب شیت را کاهش می‌دهد، به همین جهت انجام یک عملیات حرارتی مناسب پس از جوش، امری اجتناب ناپذیر است. با شبیه سازی فرآیند عملیات حرارتی این نتیجه بدست آمد که عملیات حرارتی طراحی شده برای هر دو سایت بطور موثر عمل می‌کند و میزان تنش‌ها را بطور قابل ملاحظه‌ای کاهش می‌دهد. علاوه بر این با بررسی اثر ضریب تمرکز تنش در سایت ۱ و ۲ این نتیجه حاصل شد که ضریب تمرکز تنش در سایت ۱ تقریباً دو برابر سایت ۲ است که یکی از دلایل بروز خرابی بیشتر در مبدل سایت ۱ می‌باشد.

***doi**: 10.5829/ije.2019.32.01a.15*